On the Spatial Correlation in Shallow Water and its Impact on Networking Protocols

Beatrice Tomasi*, James Preisig†, and Michele Zorzi*
*Department of Information Engineering — University of Padova, Italy
†Woods Hole Oceanographic Institution — Woods Hole, (MA) USA
Email: tomasibe@dei.unipd.it, jpreisig@whoi.edu, zorzi@dei.unipd.it

***Abstract*—In this paper, we study the spatial correlation of the communications performance in a static scenario, by using the SPACE08 experimental data set. Specifically we estimate the channel quality in terms of Signal to Interference and Noise Ratio (SINR) at the output of the equalizer, at four receiving stations, which were deployed at different distances and orientations, and we compute their cross correlation both in time and in space. This experimental study on the spatial distribution of the channel quality among nodes allows us to provide insight on the performance of networking protocols. As an example, we consider three routing policies, which we compare in terms of throughput, latency and link utilization. Results show that the policy that minimizes the number of hops is optimal in this scenario.**

I. Introduction

Underwater acoustic communications make it possible to explore and constantly monitor the ocean, wirelessly and without jeopardizing human lives, and therefore represent one of the most important technologies for ocean-related sciences and military applications. Nevertheless, they are characterized by more challenging propagation conditions than terrestrial radio communications, so as to make the optimal solutions developed for the latter unsuitable for underwater acoustic communication systems. In recent years, the scientific and military communities have also shown interest in the potential of an underwater network of sensor nodes, able to communicate with each other in order to convey the required information to a final user, safe onshore. For this reason, researchers have been investigating and designing new network protocols, optimized for the underwater acoustic scenario.

First, in order to design better protocols, the characteristics of underwater acoustic propagation which most significantly impact communications performance, have to be identified. Among these features, we enumerate the propagation delay, the time-variability and the frequency-selectivity. Moreover, from the network point of view, the spatial dimension and in particular the relationship in space between simultaneous communications performance matters. As examples, authors in [1], [2] exploit the spatial information in their routing protocols. Furthermore, the spatial relationship of the communication performance is very important in the context of mobile devices. For these reasons, in this work we study the spatial correlation of the communication performance measured at four receiving stations deployed in shallow water, 200 m and 1000 m from the transmitter along orthogonal directions. This data set has been collected during the Surface Processes and Acoustic Communications Experiment (SPACE08), which was conducted at the Martha's Vineyard Coastal Observatory (MVCO) operated by WHOI.

In the literature, works such as [3], [4], [5], [6], mainly focus on the decorrelation distance of the instantaneous channel impulse responses in terms of number of wavelengths. These results are useful for developing better receivers, but they do not provide much insight from a network perspective. Instead, here we want to understand whether different links are characterized by independent communication performance, and if not, we want to investigate how to use this correlation. We also evaluate the time series of the spatial correlation across several days and different environmental conditions, so as to qualitatively explain the observed fluctuations. In order to show how important the spatial relationship of the communication performance is for network protocols, we provide a comparative study of three different routing policies. By exploiting the measured data, we derive the performance of these routing policies in terms of throughput and latency. Results confirm that thanks to the spatial characteristics of the underwater acoustic communication performance, the policy that minimizes the number of hops is optimal in the considered scenario.

II. Scenario and System Model

In this section, the experimental conditions are detailed and their applicability to conditions in more general shallow water environments is described. In addition, we present the communications system model from which channel quality and communications performance metrics are derived.

A. Scenario

The considered scenario consists of one transmitter and four fixed receiving stations, which we call S3, S4, S5 and S6. Systems S3 and S5 are deployed along the Southeast direction at 200 and 1000 m, respectively, whereas S4 and S6 are deployed along the Southwest direction, again at 200 and 1000 m. The seafloor at the experiment site was 15 m deep, and relatively flat. The sound speed profile can be approximated as constant over the water column. In this shallow water scenario, the propagation of the sound waves is mainly affected by the interaction between the acoustic waves and the time-varying surface. Since the SPACE08 data set

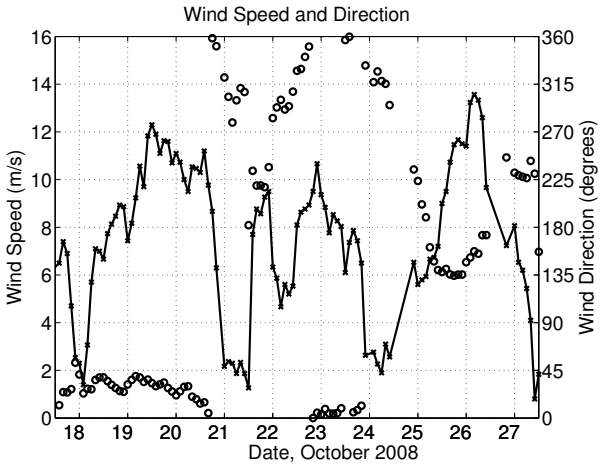

Fig. 1. Time series of wind speed and direction.

covers a broad range of wind and therefore surface conditions, it can be taken as representative of the acoustic properties of other coastal very shallow water scenarios, to which our study can be extended. As an example of the measured wind conditions, we show Figure 1, where the line represents the wind speed and the dots refer to the wind direction. The wind speed is known to influence both the noise level and the wave heights, which in turn affect the channel quality. In the following, we will consider a subset of the collected data, from October 18 to 24.

The source was omnidirectional, placed on a tripod deployed on the sea floor. The receiving stations consist of several hydrophones, recording the data. We consider here the signals collected at four hydrophones separated by $5\,\mathrm{cm}$ at S3 and S4, whereas they are separated by $12\,\mathrm{cm}$ at S5 and S6.

The transmitted acoustic signals consist of multiple repetitions of a 4095 point binary maximum length sequence transmitted at a symbol rate of 6.5 kbps and modulated according to a Binary Phase Shift Keying (BPSK) scheme at a central frequency of 12.5 kHz. A transmission one minute long was repeated successively for three times, thus resulting into a train three minutes in duration, which was sent once every two hours for ten days. From the recorded acoustic signals, we infer the channel quality and the communications performance of the communications system, described in the following section.

B. System model

Figure 2 represents the considered receiver. Modulation symbols, $a(n)$, are transmitted over the channel, $c(t,\tau)$, which introduces distortion, and they are received with additive noise $w(t)$ at the receiver side at the considered four hydrophones. After synchronization, the received signals are resampled, and processed by a Decision Feedback Equalizer (DFE), which compensates for the Inter-Symbol Interference (ISI). The DFE is adapted in a training mode, with Bit Error Rate (BER) and SINR statistics calculated using the data that follows an initialization period of 2000 symbols. The output of the

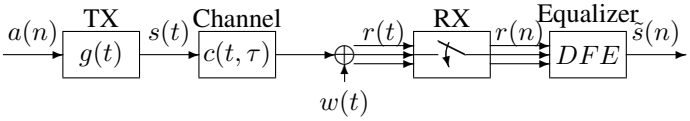

Fig. 2. System model. The symbol $r(t)$ represents the vector of the received symbols at different receiver elements.

equalizer, the software decision, is then decoded into symbols by using a minimum distance criterion.

We subdivide the received signal into packets, consisting of 6500 symbols, of which 2000 are used for the initialization of the equalizer. We then measure the number of symbols which were not correctly received per packet, thus obtaining the communication performance in terms of BER for every average SINR measured at each packet.

The software decision, $\tilde{s}(n)$ can be expressed as:

$$\tilde{s}(n) = a(n) + \tilde{w}(n), \tag{1}$$

where $\tilde{w}$ is the residual additive noise, which includes noise and residual ISI, and $a(n)$ is the transmitted symbol. The statistical power of the residual noise $\tilde{w}$, indicated as σ^2, can be estimated over the information symbols in a packet as

$$\sigma^2 = \frac{1}{N-1}\sum_{n=1}^{N} |\tilde{s}(n) - a(n)|^2. \tag{2}$$

The SINR, indicated as γ, is computed as $\gamma = \frac{E_s}{\sigma^2}$, where E_s is the average symbol energy.

III. Spatial correlation coefficient

In this section, we present the estimated average channel quality in terms of SINR and the corresponding communications performance in terms of BER. Then, we show the spatial correlation coefficient of the channel quality among the four receiving stations.

A. SINR and communications performance

We present and discuss the obtained time series of the SINR, averaged over each packet and measured at the output of the equalizer. Fig. 3 presents the SINR time series at systems S4 and S6, which were deployed along the same direction, but at 200 and $1000\,\mathrm{m}$ from the transmitter. The time series refer to the period from October 18 to 24, and the same observations hold for the SINR time series observed at S3 and S5.

We notice that the levels of SINR are quite comparable during the experiment period, even though the receivers are separated by $800\,\mathrm{m}$. This can be explained by observing Fig. 4 in which we show an example of the measured amplitude of the channel impulse response measured on October 22 at receivers S4 and S6. The figure shows that the impulse response for the S4 channel has a significantly greater delay spread than the S6 channel. Therefore, even though the signal to S4 experiences lower average attenuation due to the shorter range, it experiences greater ISI, which is not completely eliminated by the DFE. This balance between the signal level and the ISI effects results into SINRs that are comparable

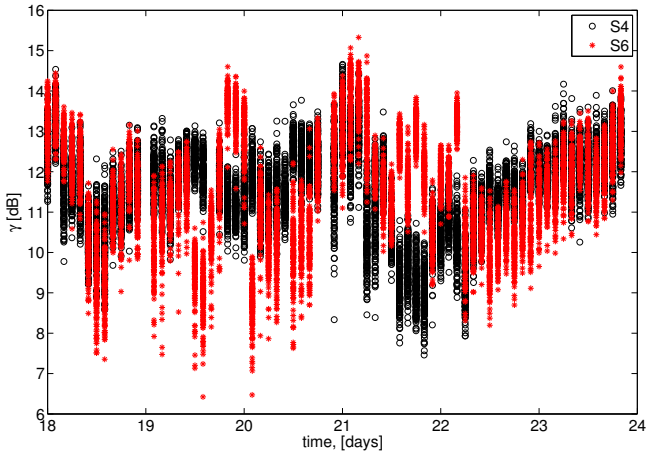

Fig. 3. Time series of the measured average SINR at systems S4 and S6, from October 18 to 24. We recall that the presented estimates are taken every two hours for three minutes, during each day.

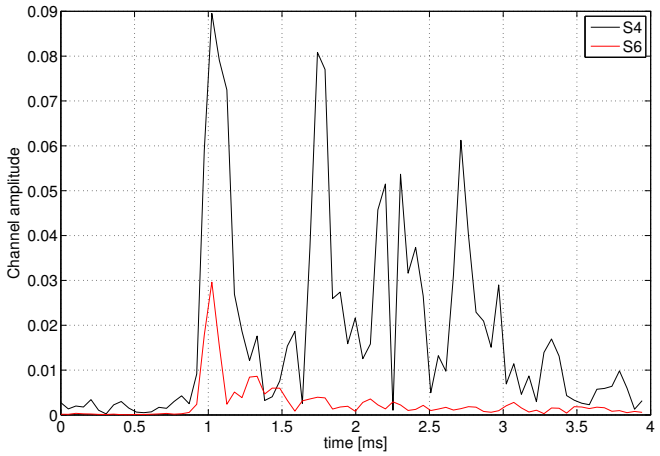

Fig. 4. Examples of the amplitude of the channel impulse response at systems S4 and S6, during October 22.

between the links from the transmitter to S3 and S4 (and similarly from the transmitter to S5 and S6).

The figure shows that the impulse response for the S4 channel has a significantly greater delay spread than the S6 channel. Therefore, even though the signal to S6 experiences greater attenuation due to the longer range, it also experiences greater ISI. The ISI is not completely eliminated by the DFE. The balance of the lower signal level and ISI effects result into SINRs that are comparable between S3 and S4 and S5 and S6.

Since the levels of SINR values are in the medium-high range (around 7 to 14 dB), the observed BER is quite low. In order to provide the overall communications performance, we show in Fig. 5 the time series of the BER averaged over the three minute interval, from October 18 to 24, for stations S4 and S6. As observed before for the SINR, the communications performance of the longer link is comparable with (and sometimes even slightly better than) that of the shorter one. This observation also holds for systems S3 and S5.

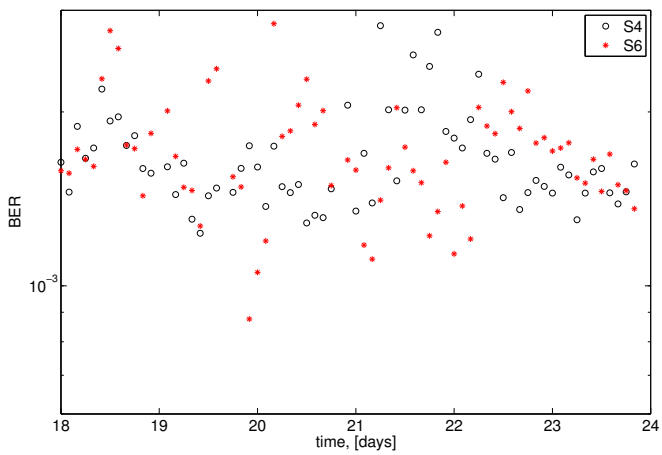

Fig. 5. Time series of the observed average BER at systems S4 (black points) and S6 (red points).

The observations in this section motivate the study that will be presented in Section IV, where we will evaluate the performance of different routing policies. Indeed, unlike in terrestrial wireless networks, where shorter links are typically more reliable and therefore often preferred in a routing algorithm, in the scenario under study long and short links have comparable communications performance, so that a different paradigm should be used. This is why we are also interested in studying the spatial correlation of the measured average SINR among the nodes, which is provided in the next section.

B. Spatial correlation coefficient

The spatial correlation coefficient between two receivers, S_i and S_j, is computed as

$$\rho\left(S_i, S_j\right) = \frac{Cov(\gamma_i, \gamma_j(\tau))}{\sqrt{Cov(\gamma_i)C(\gamma_j(\tau))}}, \tag{3}$$

where $Cov(\cdot)$ is the covariance function defined as $Cov(x,y) = \mathbb{E}[(x-m_x)(y-m_y)]$ and τ represents the difference between the propagation delays from the source to stations S_i and S_j. The covariance is estimated by $Cov(\gamma_i, \gamma_j) = \frac{1}{N-1}\sum_{n=1}^{N}(\gamma_i(n)-m_i)(\gamma_j(n+\tau)-m_j)$, where m_i and m_j are the SINRs averaged over the time interval three minutes long at S_i and S_j. In this way, we obtain a temporal behavior of the spatial correlation coefficient, $\rho(t)$.

We study the time series of the correlation coefficient, since we want to understand whether or not it depends on environmental conditions, which are also time-varying. We want to highlight that the estimated coefficient, as indicated in Eq. (3), indicates how the trends of the SINRs, measured at stations S_i and S_j, are correlated, e.g., whether the SINR is increasing (decreasing) at S_i, when it is increasing (decreasing) at S_j. The case of sufficiently high correlation coefficient can be useful when the transmitter knows the channel state information on

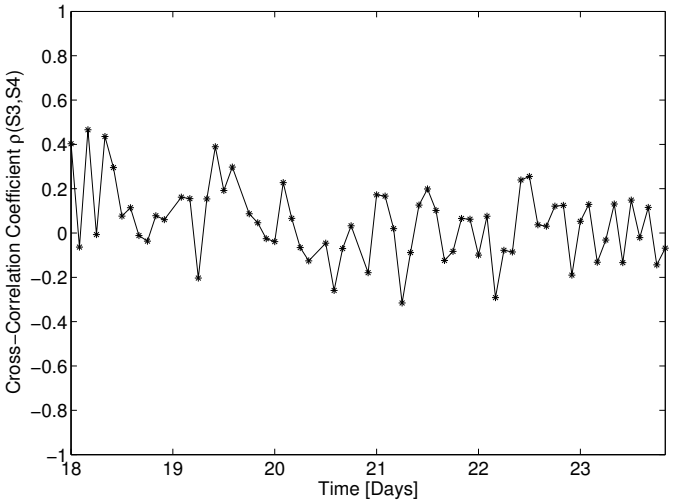

Fig. 6. Spatial correlation between systems S3 and S4, deployed at 200 m.

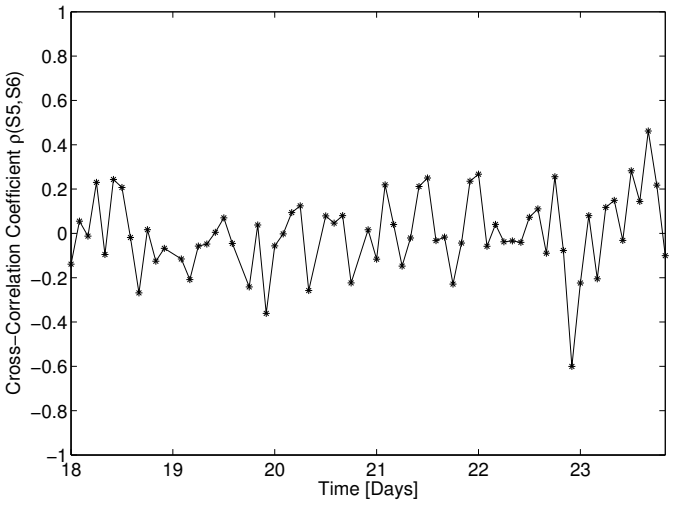

Fig. 7. Spatial correlation between systems S5 and S6, deployed at 1000 m.

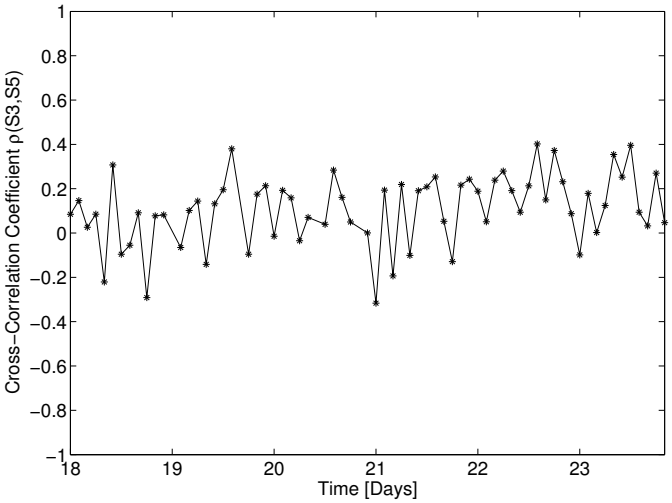

Fig. 8. Spatial correlation between systems S3 and S5, deployed along the Southeast direction.

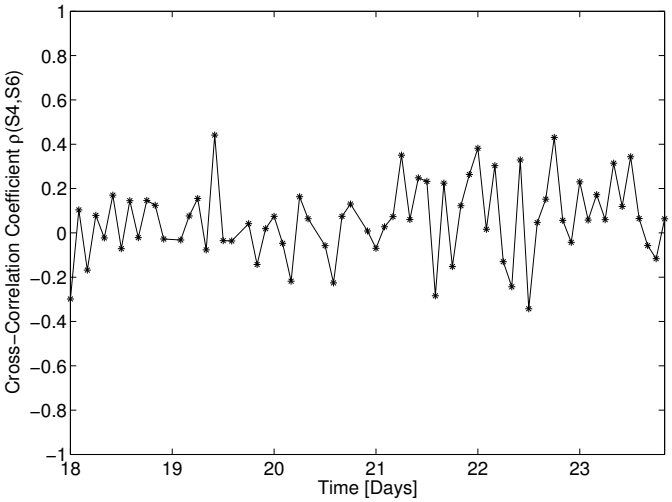

Fig. 9. Spatial correlation between systems S4 and S6, deployed along the Southwest direction.

S_i and wants to infer some information about the channel state at S_j.

In Fig. 6, we show the time series of the correlation coefficient for the couple (S3,S4), in order to investigate how correlated the SINRs measured along orthogonal directions are for the shorter links. We observe rather low correlation levels over the whole observation period.

In Fig. 7, which represents the cross-correlation coefficient between S5 and S6, we can observe a similar behavior.

Fig. 8 shows the time series of the correlation coefficient between S3 and S5, deployed along the same direction but at different distances. These results quantify how correlated the channel quality is at different distances. A high correlation means that the trends around the average during the three minutes of observation are very similar at the shorter and longer links, thus suggesting that the fluctuations of the SINR are caused more by the direct arrivals than by the surface reflected arrivals.

For completeness we also present Figs. 9, 10, and 11, which show the time series of the spatial correlation coefficient between S4–S6, S3–S6, and S4-S5 respectively.

In Fig. 12 we present a case of correlated SINR measured at S3 and S6. In fact, we can notice that when the SINR at S3 decreases with respect to the average in the three minute interval, the SINR at S6 follows the same trend. Conversely, in Fig. 13, we show a case of non correlated SINRs, in which the time series exhibits an i.i.d. behavior for both systems S4 and S6.

To conclude, we discuss on the importance of the presented results. We have shown that in a very shallow water scenario the channel quality seen above the physical layer is comparable at different ranges, and that the trends of this quality are rarely similar across the experiment area. This result can be very useful in networking protocols and in mobile scenarios, since if the channel quality is known at a short distance, it can be

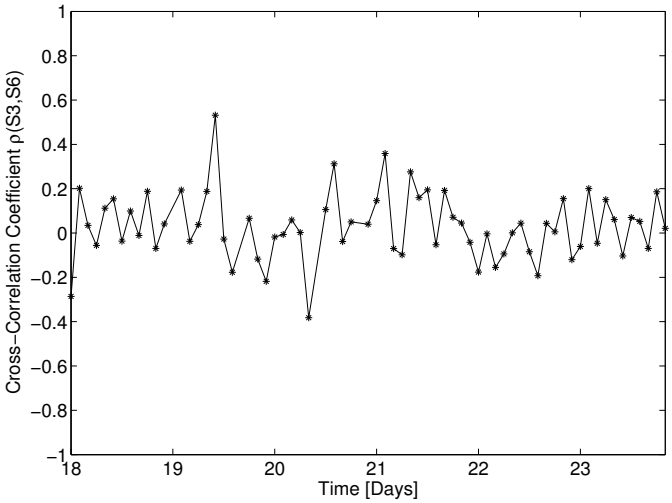

Fig. 10. Spatial correlation between systems S3 and S6.

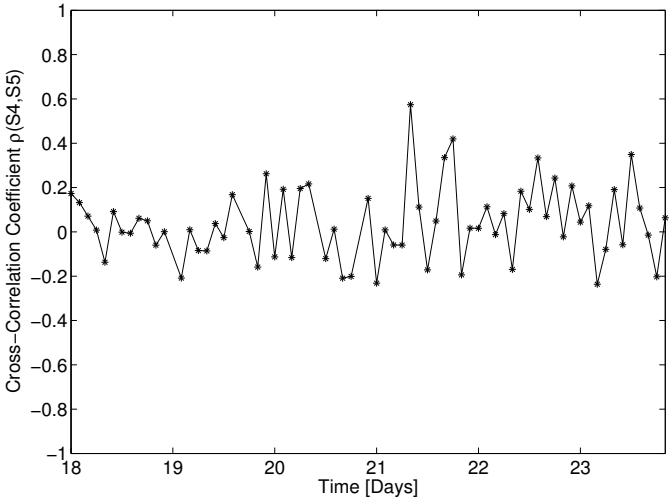

Fig. 11. Spatial correlation between systems S4 and S5.

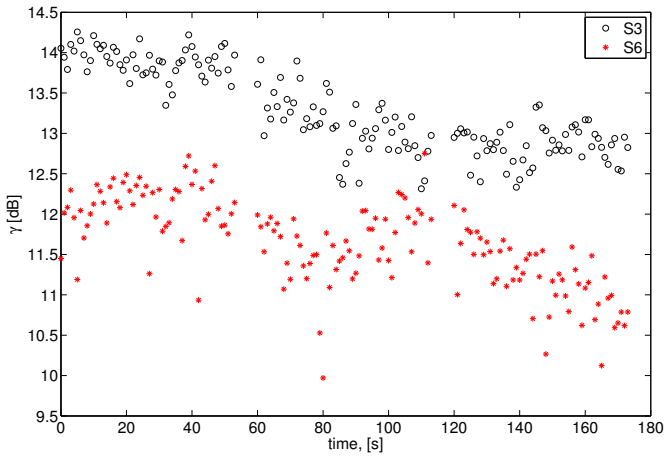

Fig. 12. Time series of the SINR measured at S3 and S6 during the three minute interval at noon, October 19, when the correlation coefficient is close to 0.6.

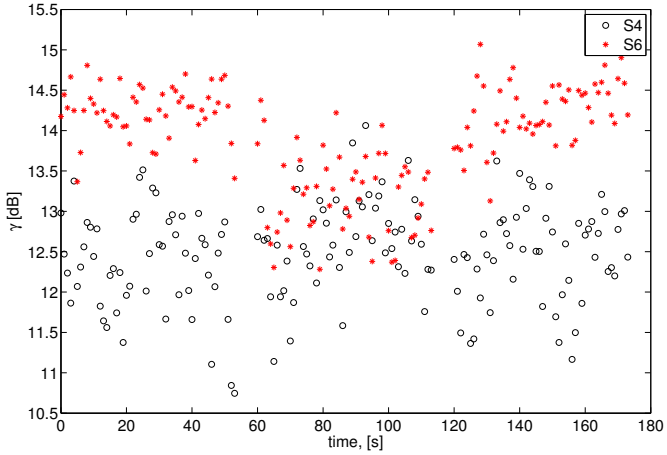

Fig. 13. Time series of the SINR measured at S4 and S6 during the three minute interval at 4 am, October 21, when the correlation coefficient is small.

assumed to be similar in the longer distance and if the channel quality trend is decreasing then, under certain conditions, the same behavior can be expected on the longer link. To provide further evidence about these conclusions, in the next Section we show a study on routing policies.

IV. Evaluation of routing policies

In light of what was presented so far, we now describe the considered static network and three routing policies, which we will evaluate in terms of performance and link utilization by using the processed data. The main objectives of this study are to evaluate and compare three routing policies in the static shallow water scenario, in order to understand whether an optimal policy exists in such case. In order to carry out this evaluation, we assume the network topology shown in Figure 14, where the source node S has to transmit data to a destination node, denoted as D, through the relay nodes S3, S4, S5 and S6. We also assume that node D is sufficiently far from the source node S (say 2000 m), so that they cannot communicate directly with each other. Analogously, we assume that only S5 and S6 can reliably communicate with D.

Moreover, since the data from S3 to S5 and S6, and the data from S4 to S5 and S6 are not available and given that the distances are similar to those from S to S5 or from S to S6, we assume that the channel quality of these links is the same as that measured between the source node S and the receiving stations S5 and S6. Another approach could be to consider the spatial correlation coefficient between the couples (S3,S5), (S3,S6), (S4,S5) and (S4, S6) at the proper delays, and infer the missing data by exploiting the correlation. However, we employ the first approach since in this way we can use the entire time series and not only the data during periods with high correlation coefficients. Moreover this approach is a reasonable approximation, since we observed similar performance between the shorter and longer links.

From this assumption, we can expect that the longer links

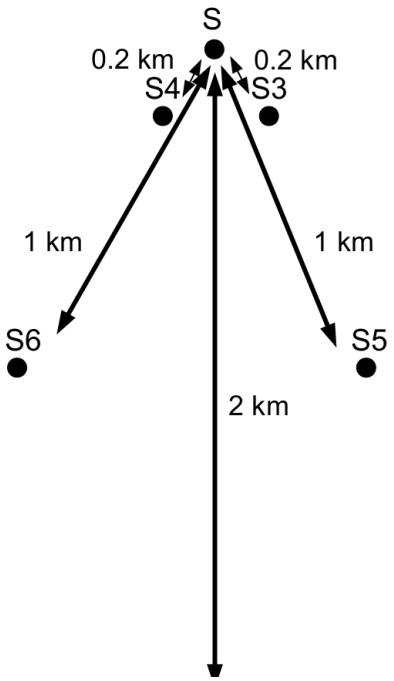

Fig. 14. Considered scenario.

are the best choice in a routing protocol for this shallow water scenario, since passing through the relaying nodes at the shorter links does not provide any advantage, in terms of reliability, and will incur higher latency. However, since in the simulation we downsample the SINR time series between S and S5 or S6 at different rates depending on whether we consider links S to S5 (S6) or S3 (S4) to S5 (S6), we show this same result obtained via simulation. We also assume that links S5–D and S6–D are fully reliable, i.e., once the packet reaches S5 or S6, it is reliably delivered to the destination.

The first considered policy is the most general among those we evaluate. In fact, it consists in choosing the path that maximizes the minimum per-hop SINR, thus resulting in the optimal policy in terms of reliability, since it maximizes the communications performance of the network bottleneck. For this policy the possible paths from the transmitter to the destination are six, i.e., $p \in A = \{$ S–S3–S5–D, S–S3–S6–D, S–S4–S5–D, S–S4–S6–D, S–S5–D, S–S6–D $\}$ and the chosen path can be expressed as

$$\hat{P1} = \arg\max_{p \in A} \gamma(p), \tag{4}$$

where $\gamma(p)$ is the minimum SINR measured over all hops in path p.

The second policy consists in restricting the above search to paths with the minimum number of hops. In this case the possible paths are a subset of A, i.e., $p \in B = \{$ S–S5–D, S–S6–D $\}$ and the chosen path can be written as

$$\hat{P2} = \arg\max_{p \in B} \gamma(p). \tag{5}$$

The third policy is also a particular case of the first one, and it limits the first search to paths with the shortest hops. In this case the possible paths are a subset of A, i.e., $p \in C = \{$ S–S3–S5–D, S–S3–S6–D, S–S4–S5–D, S–S4–S6–D$\}$ and the chosen one is

$$\hat{P3} = \arg\max_{p \in C} \gamma(p). \tag{6}$$

When running the simulations, we downsample the time series of the measured γ at the proper propagation delays for the different links and we consider the communications performance and the delay associated at each hop for all possible paths in each policy. In this way, we could then evaluate the throughput, the latency to deliver the packet, and the percentage of the link utilization.

We compute the throughput as the fraction of correctly received bits per unit time. The time unit is the time to transmit a packet, which is almost 1 s. If a packet is not correctly received at any hop in the path it is dropped. The latency delay is the time spent by the packet in order to reach the destination, which depends on the length of the packet, which is fixed, on the propagation delay, and on the hops chosen by the policy. Eventually, we also evaluate the number of times a link was chosen by each policy in order to observe whether there exists a privileged direction.

Table I shows the results averaged over the period from October 18 to 24. In the considered scenario, the first and second policy are equivalent, and are optimal in terms of both latency and throughput. This confirms the results presented in Section III-B, where we showed that the channel quality of the longer links is comparable to that of the shorter links, and for this reason the policy which minimizes the number of hops has also the best performance in terms of reliability. However, the second policy is simpler to implement, since it does not require information on the channel quality to be fed back for all the available links, but only for the local ones, in this case S5 and S6. On the other hand, we note that the whole topology still needs to be known by all nodes in the network, in order to be able to compute the path that has the minimum number of hops. This shared knowledge of the topology might be a problem in mobile networks, whereas in static networks it has to be recomputed only in case of link failures.

As a final remark, we highlight that the obtained results are valid in a very shallow water scenario, for which the channel quality only depends on the surface conditions, whereas for shallow water scenarios for which the water column is around 100 m a further study should be performed, since for those conditions it is not well understood how the combination of time-varying sound speed profile and surface conditions affect the channel quality in the horizontal space. Studies such as [7], [8], [9], [10] have investigated the impact of the environmental variability on the channel quality in the vertical space, but the horizontal space contribution has not been provided yet, and will be part of our future work.

V. Conclusion

In this paper, we studied the horizontal spatial correlation of the channel quality by using experimental data collected in a

TABLE I
POLICY EVALUATION

Policy vs Performance	Policy 1	Policy 2	Policy 3
Throughput kbps	4.4409	4.4409	4.4393
Latency s	1.333	1.333	1.43
S3–S5	0	0	0.1701
S4–S6	0	0	0.2754
S5	0.4943	0.4943	0
S6	0.5057	0.5057	0
cross links	0	0	0.5545

very shallow water scenario. Then, based on the observations derived in the first part of the paper, we evaluated three policies which are usually employed in routing protocols. We computed their average performance in terms of throughput, latency and link utilization.

Results on the spatial correlation study show that short ($200\,\mathrm{m}$) and long ($1000\,\mathrm{m}$) links have comparable channel quality from a BPSK communications system perspective. Moreover, in light of what observed for the spatial correlation, we have shown that the optimal routing policy is the one that minimizes the number of hops.

This study made it possible to better understand the spatial dynamics of the channel quality, for a specific but usual scenario in coastal areas. Further similar studies will be carried out in order to better understand the spatial distribution of the channel quality in underwater acoustic networks in deeper water, so that more efficient networking protocols can be designed.

ACKNOWLEDGMENT

This work has been supported by ONR under Grants no. N00014-05-10085 and N00014-10-10422 and by the European Commission under the Seventh Framework Programme (Grant Agreement 258359 – CLAM).

REFERENCES

[1] M. Zorzi, P. Casari, N. Baldo, and A. Harris, "Energy-efficient routing schemes for underwater acoustic networks," *IEEE Journal on Selected Areas in Communications*, vol. 26, no. 9, pp. 1754 –1766, December 2008.

[2] J. M. Jornet, M. Stojanovic, and M. Zorzi, "Focused beam routing protocol for underwater acoustic networks," in *Proceedings of the third ACM international workshop on Underwater Networks*, 2008, pp. 75–82.

[3] O. Galkin and S. Pankova, "Correlation of underwater acoustic signals simultaneously received by omnidirectional and directional means," *Acoustical Physics*, vol. 54, pp. 337–345, 2008.

[4] J. Cross and Y. R. Zheng, "Impact of Spatial Correlation of Fading Channels on the Performance of MIMO Underwater Communications," in *Proceedings of the IEEE Military Commun. (Milcom11)*, Nov. 2011, pp. 1–5.

[5] H. Guo, A. Abdi, A. Song, and M. Badiey, "Correlations in underwater acoustic particle velocity and pressure channels," in *43rd Annual Conference on Information Sciences and Systems, CISS*, Mar. 2009, pp. 913 –918.

[6] A. Zajic, "Statistical space-time-frequency characterization of MIMO shallow water acoustic channels," in *MTS/IEEE OCEANS 2009, Biloxi*, Oct. 2009, pp. 1 –6.

[7] A. Song, M. Badiey, H. C. Song, and W. S. Hodgkiss, "Impact of source depth on coherent underwater acoustic communications," *The Journal of the Acoustical Society of America*, vol. 128, no. 2, pp. 555–558, 2010.

[8] T. C. Yang, "Properties of underwater acoustic communication channels in shallow water," *The Journal of the Acoustical Society of America*, vol. 131, no. 1, pp. 129–145, 2012.

[9] A. Song, M. Badiey, H. C. Song, W. S. Hodgkiss, M. B. Porter, and the KauaiEx Group, "Impact of ocean variability on coherent underwater acoustic communications during the Kauai experiment (KauaiEx)," *The Journal of the Acoustical Society of America*, vol. 123, no. 2, pp. 856–865, 2008.

[10] M. Badiey, Y. Mu, J. Simmen, and S. Forsythe, "Signal variability in shallow-water sound channels," *IEEE Journal of Oceanic Engineering*, vol. 25, no. 4, pp. 492 –500, Oct. 2000.